Study of γ-Alumina Surface Reactivity: Adsorption of Water and Hydrogen Sulfide on Octahedral Aluminum Sites

Andrei Ionescu, Alain Allouche,* Jean-Pierre Aycard, and Michel Rajzmann

Physique des Interactions Ioniques et Moléculaires, UMR 6633, and University of Provence, rue Escadrille Normandie Niemen, 13397, Marseille Cedex 20 France

François Hutschka

TotalFinaElf, CERT, BP 27, 76700 Harfleur, France

Received: January 17, 2002; In Final Form: April 10, 2002

We report on a study of adsorption of probe molecules on the aluminum sites of γ-alumina surface planes. DFT electronic structure and total energy calculations for (100) and (110D) surface planes were carried out in order to find the reactive sites. The adsorption of two molecular species (water and hydrogen sulfide) was studied using a DFT plane-wave pseudopotential method. We found that both molecules were adsorbed on the (100) surface and that both molecules were dissociated on the (110D) surface. Consequently, the (110D) surface is more reactive than the (100) surface.

1. Introduction

Aluminas are widely used as adsorbents and active catalysts as well as catalyst supports for a number of technological applications.[1] We were interested in the study of γ-alumina reactivity because of its use as a catalyst support in the refining industry.[2,3] Its advantages are mechanical and high temperature resistance and especially its acid−base properties.[1,4]

The cobalt oxide/molybdenum oxide/alumina is extensively used as a catalytic system for hydrodesulfurization, hydrodenitrogenation, and hydrocracking reactions.[4]

Our focus is the hydrodesulfurization (HDS) process, used to produce fuels (diesel and gasoline) with greatly reduced levels of sulfur. The HDS reaction is catalyzed by well-dispersed molybdenum sulfide nanocrystallites supported on γ-alumina and promoted by cobalt or nickel atoms.[5−7] Despite its application, there is limited understanding of the real interaction between the catalyst and the support. To better understand this interaction, we investigated the reactivity of γ-alumina by using two probe molecules (water and hydrogen sulfide). The present work makes use of our previous results[8,9] on this subject and broadens the analysis by using new quantum methods.

γ-Alumina has a spinel-like structure ($MgAl_2O_4$) in which the magnesium atoms are substituted by aluminum atoms.[10] The oxygen lattice is built up by a cubic close-packed stacking of oxygen layers and aluminum atoms occupy octahedral and tetrahedral sites. Thus, an ideal spinel-type unit cell consists of 56 atoms (32 oxygen and 24 aluminum atoms, 16 octahedral and 8 tetrahedral). The stoichiometry of γ-alumina does not fit the spinel-like structure. There are $2^2/_3$ vacant cation positions per unit cell and the unit cell contains 32 oxygen atoms and $21^1/_3$ aluminum atoms in order to satisfy the γ-Al_2O_3 stoichiometry.[11] There is controversy concerning the exact localization of vacancies. Experimental studies such as X-ray diffraction (XRD),[12] nuclear magnetic resonance (NMR),[13,14] and neutron scattering[15] have shown contradictory results: vacancies are believed to occupy either octahedral or tetrahedral positions. Some studies consider even that there are cations occupying sites which are vacant in the ideal spinel structure.[15] See ref 16 for a detailed description of spinel-based transition aluminas. Recent theoretical studies have calculated that, for the bulk, vacancies in the octahedral sites are energetically preferred.[16,17] As for our models of the surface, the stoichiometry depends on the direction of cleaving, the number of layers, and the dimension of unit cell. Some surfaces are stoichiometric and ideal, and some must contain vacancies in order to become stoichiometric.

Numerous experimental studies have investigated the surface of γ-alumina. By means of vibrational spectroscopy, the surface configuration was deducted from the IR spectra of the surface hydroxyls.[18−22] One of the first models[23] considered that the active surface is represented only by the (100) plane. The (100) surface exposes a cubic lattice of close-packed oxygen atoms with only octahedral aluminum atoms present in between. Other models[4,19] considered that the representative surface is the (110) surface, which exposes two types of layers: C and D layers depending on the cations distribution. The C layer exposes both octahedral and tetrahedral aluminum atoms. The D layer exposes only octahedral aluminum atoms. Both layers expose tricoordinated oxygen atoms.

From an experimental standpoint, the surface reactivity of γ-alumina was investigated via adsorption of molecules such as water,[24] hydrogen, oxygen, carbon monoxide, and carbon dioxide,[25,26] as well as hydrogen sulfide[27].

Numerous theoretical levels were employed. First, there were molecular dynamics (MD) simulations of transition aluminas,[28,29,30] which generally investigated both the surface and the bulk structures. The electronic structure of alumina surface was investigated by means of the periodic Hartree−Fock method in statically relaxed geometries.[31] Quantum chemical studies were also used in order to investigate the acid−base nature and the local surface structure.[32,33] The reconstruction of the (110) surface[34] was investigated by means of density functional calculations coupled with plane wave basis (DFT-PW). Other works have focused on the reactivity studies of γ-alumina sites in interaction with small molecules such as HCl,[35] CO,[36,8] H_2O,[8,37] H_2S,[8] CH_3OH,[38] MoS_2,[39] and $(Re)_2(CO)_{10}$.[40]

* To whom correspondence should be addressed. Alain.Allouche@piimsdm.univ-mrs.fr.

10.1021/jp020145n CCC: $22.00
Published on Web 08/15/2002

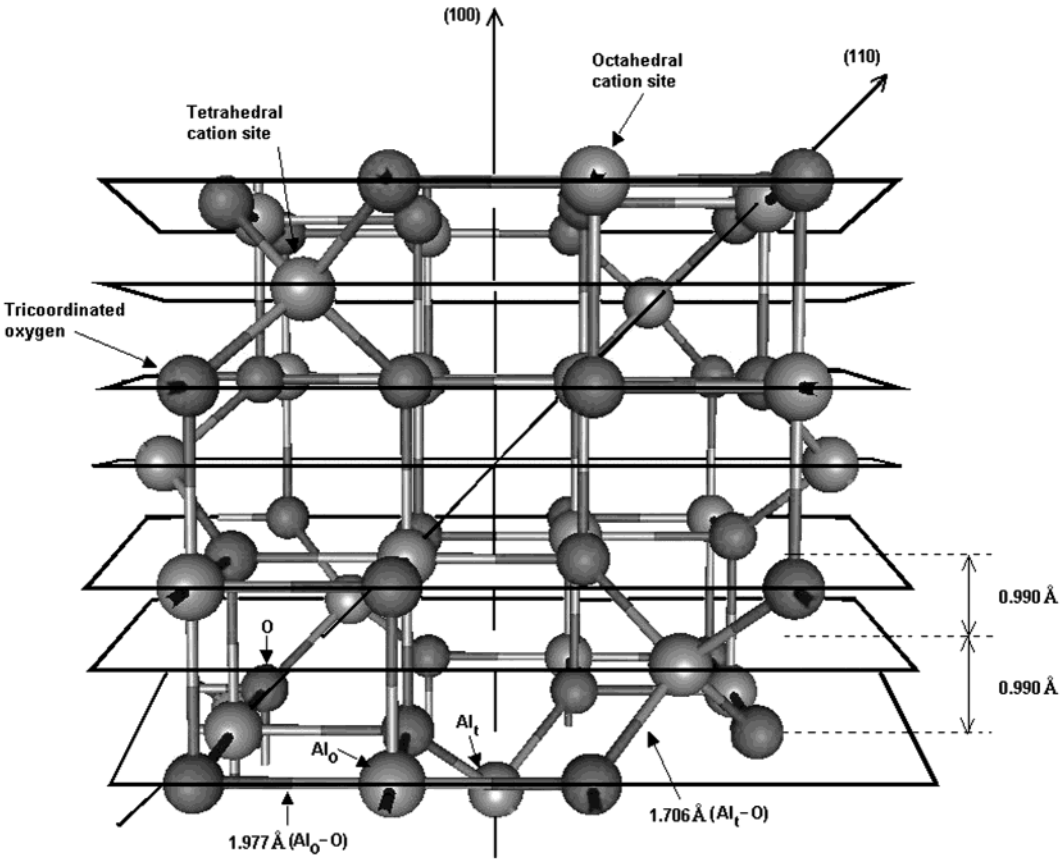

Figure 1. γ-Alumina spinel-type unit cell.

Under atmospheric conditions, the surface of γ-alumina adsorbs water both molecularly and dissociatively, thus creating hydroxyl groups on the surface. It has been shown that the surface hydroxyl groups have five possible configurations,[4] as suggested by the five IR bands detected, and there were at most four different kinds of OH groups on the surface if one assumes that only the (100) and (110) surfaces were exposed. However, more recent papers[41,42,19] suggest more than five OH bands in the IR spectra. It is also important to understand the interaction between H_2S and γ-alumina surface because hydrogen sulfide is present during the hydrodesulfurization reaction.

In the present study, we investigated the reactivity of acid octahedral surface sites of the (100) face and of the (110D) face. The (110C) face exposes both octahedral and tetrahedral aluminum atoms. As shown by previous studies,[30,34] the (110C) layer is energetically preferred but suffers important reconstruction resulting in the loss of Al from surface tetrahedral cation positions. Consequently, the reconstruction eliminates the three-coordinated Al atoms of the surface leaving only four-coordinated Al atoms similar to the (110D) layer. As our model was mainly based on the structural features extracted from the ideal bulk, no vacancies were imposed on the surface layers, and we believe that the choice of (100) and (110D) layers is rigorous and describes the reactive sites of alumina surfaces. We conducted calculations on stoichiometric and nonstoichiometric surface planes. The study of bare surface relaxation preceded the adsorption of molecular systems.

2. Computational Method

Periodical plane-wave DFT calculations were applied within the generalized gradient approximation in the Perdew−Wang functional.[43,44] We used nonlocal reciprocal-space pseudopotentials in the Kleinman−Bylander form.[45] The plane wave cutoff energy was 420 eV. Calculations were done for a Monkhorst Pack grid,[46,47] for the Brillouin zone integration of k points, with 0.1 Å^{-1} spacing. All calculations were done with the CASTEP[48] code. The standard band width for all gaussian representations of total DOS and atom-resolved PDOS was 0.2 eV.

TABLE 1: Lattice Parameters of the Considered Unit Cells

unit cell	parameters
(100) five-layer slab	$a = 18.9$, $b = c = 5.6$ Å, and $\alpha = \beta = \gamma = 90°$
(110D) four-layer slab	$a = 19.1$, $b = 7.9$, $c = 5.6$ Å, and $\alpha = \beta = \gamma = 90°$
(110D) six-layer slab	$a = 21.9$, $b = 7.9$, $c = 5.6$ Å, and $\alpha = \beta = \gamma = 90°$

Three surfaces were generated from the experimental cubic unit cell (Figure 1) of γ-alumina. The (100) surface was modeled by a five-layer stoichiometric spinel-type slab of 20 atoms (12 oxygens and 8 aluminum atoms). The (110D) surface was modeled by two slabs: a four-layer nonstoichiometric spinel-type slab of 28 atoms (16 oxygens and 12 aluminum atoms) and a six-layer stoichiometric defective slab of 40 atoms (24 oxygens and 16 aluminum atoms). Two vacant cation positions were placed in the bottom layer of the latter slab in order to satisfy the γ-alumina stoichiometry. The ideal nonstoichiometric four-layer surface provided an alternative for the stoichiometric six-layer surface because of the computational time limitations induced by the relaxation of the latter surface. As a consequence, we studied the relaxation of only the four-layer (110D) slab. The lattice parameters of all three unit cells are shown in Table 1. We imposed a vacuum of 15 Å between slabs in the a direction of the crystal lattice, which is perpendicular to the surface plane and then periodically repeated the unit cell throughout space.

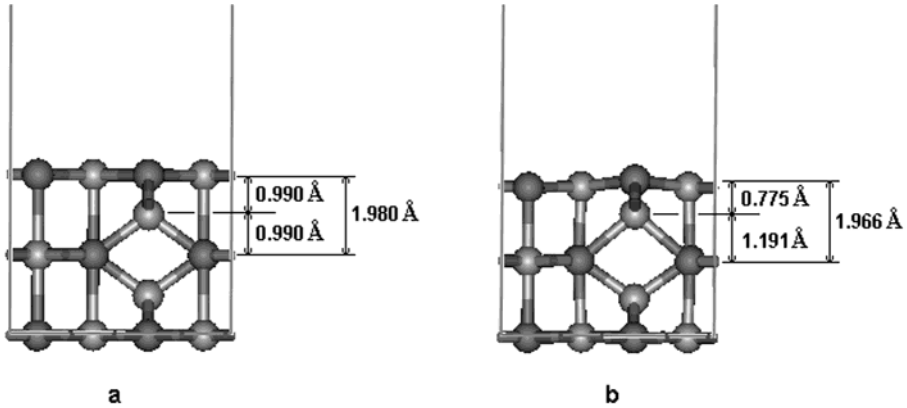

Figure 2. Geometry of γ-alumina (100) unit cell before (a) and after (b) relaxation.

TABLE 2: Bond Lengths (Å) for the (100) Surface Plane

bond length	fixed 5-layer slab	optimized 5-layer slab1[a]
Al_O-O	1.976	1.802−1.949
Al_t-O	1.706	1.737−1.846

[a] Upper 3 layers optimized and bottom two layers fixed.

Two approaches were considered in order to evaluate the influence of surface relaxation on the γ-alumina chemical reactivity. In the first approach, we relaxed the geometry of the adsorbed molecules while all surface layers were frozen. In the second approach, we relaxed the adsorbed molecules and the upper three layers while the remaining layers were frozen. In all cases, the cell parameters were kept frozen. The adsorption and dissociation energies were calculated as follows:

$$E_{ads/diss} = E_{(Molecule+Surface)} - E_{(Surface)} - E_{(Molecule)} \quad (1)$$

where $E_{(Molecule+Surface)}$ refers to the energy of the system formed by the adsorbed/dissociated molecule and the surface, $E_{(Surface)}$ refers to the energy of the bare surface in its equilibrium geometry, and $E_{(Molecule)}$ refers to the energy of the isolated molecule in its adsorbed geometry (adsorption) or in its optimized geometry (dissociation).

3. Results

3.1. Surface Relaxation. First, we studied the surface relaxation. Only the layer that exposed five-coordinated Al atoms and three-coordinated O atoms was considered for the (100) surface. We optimized the upper three surface layers while the bottom two layers were frozen. The equilibrium geometry of the (100) slab (Figure 2) shows that there are minor perturbations and that the initial structure of γ-alumina is well preserved.

However, the surface oxygen atoms bonded to tetrahedral aluminum atoms move above the surface with 0.158 Å. The distance between the first layer Al atoms and the third layer O atoms after relaxation is 1.966 Å. The second layer, consisting only of tetrahedral aluminum atoms, moves toward the surface. The mean distance between the first layer Al atoms and the second layer Al atom of the optimized surface is by 0.215 Å smaller than the same distance on the fixed surface (Table 2). As for the third optimized layer from the surface, the relaxation preserves its initial morphology.

The total density of states (DOS) plots (Figure 3) show that the relaxation of the surface layers induces changes in the density profile. The atom-resolved projected density of states (PDOS) plots show that the contribution of aluminum atoms to the valence band is small and more significant for the conduction

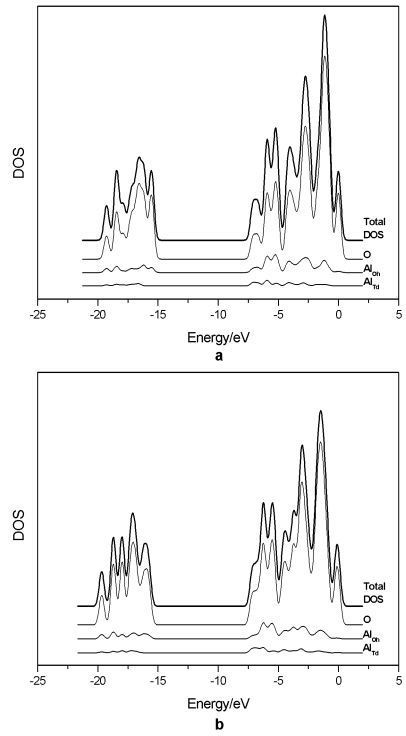

Figure 3. Electronic density of states plots of (a) unrelaxed and (b) relaxed (100) γ-alumina unit cell. Total DOS (arbitrary units) and atom-resolved PDOS for oxygens (O), octahedral (Al_{Oh}), and tetrahedral (Al_{Td}) aluminum atoms.

band. The Fermi energy is −16.081 eV in the case of the relaxed slab and −15.556 eV in the case of the unrelaxed slab. The conduction bands as well as the valence bands are situated practically in same regions before and after relaxation. The band gap for the relaxed slab is 8.921 eV, whereas it is 8.733 eV for the unrelaxed slab.

A careful examination of the valence band profiles shows that the unrelaxed surface exhibits a complicated structure where four peaks can be identified, with the third one starting from the low energy domain being a triplet. These peaks correspond to the different Al−O bonds that can be easily identified in the slab. The relaxation induces a neat splitting of the triplet, which means that the corresponding chemical bonds are differentiated. Figure 2 shows that the dissimilarities are mainly generated by the interlayer Al−O bonds.

For the four-layer nonstoichiometric (110D) surface, we optimized the three upper layers while the bottom layer was frozen. The equilibrium geometry shows that there is significant

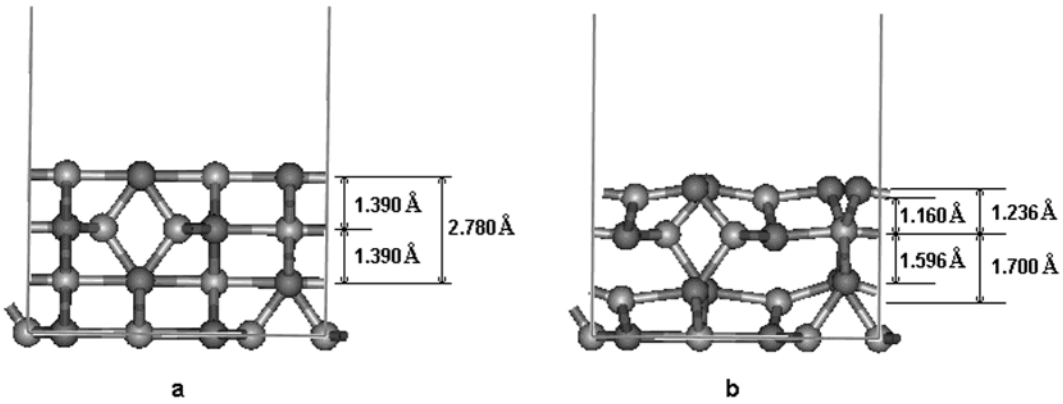

Figure 4. Geometry of γ-alumina (110D) unit cell before (a) and after (b) relaxation.

TABLE 3: Bond Lengths (Å) for the (110D) Surface Plane

bond length	fixed 4-layer slab	optimized 4-layer slab1[a]
Al_O-O	1.976	1.661−1.881
Al_t-O	1.706	1.675−1.881

[a] Upper 3 layers optimized and bottom layer fixed.

surface relaxation (Figure 4), with surface oxygen atoms moving above the ideal surface.

There is also a change in the coordination of the bulk aluminum atoms. The bond lengths between the tetrahedral Al atom of the third layer and the two four-coordinated O atoms of the second layer change from 1.976 to 2.229 Å (Table 3). The corresponding bond orders decrease from 0.30 to 0.16 electrons, and the Al electronic charge decreases from 1.51 to 1.68 electrons. As a consequence, the aluminum atom which is six-coordinated and octahedral in the ideal structure becomes four-coordinated in the optimized one.

However, this change in electron density is smaller than the change observed for the four-coordinated octahedral aluminum atoms of the first layer which increases from 1.46 to 1.85 electrons. After optimization, the charges on the four-coordinated tetrahedral and octahedral aluminum atoms of the first two layers are 1.74 and 1.85 electrons, respectively. On the fixed surface, the corresponding charges are 1.85 and 1.46 electrons. The DOSs for the unrelaxed (Figure 5a) and the relaxed (Figure 5b) surfaces reflect the perturbation of the (110D) surface after relaxation. The Fermi energy for the relaxed slab (−19.790 eV) is lower than for the unrelaxed one (−17.485 eV). The electronic profiles show a contraction of the valence band after relaxation, which induces a band gap increase from 6.339 (unrelaxed slab) to 8.969 eV (relaxed slab). The Al atoms contribution to the total DOS is weak, and the electronic profiles show that for both tetrahedral and octahedral aluminum atoms there are minor changes after relaxation. The comparison of oxygen-resolved PDOS between the relaxed and unrelaxed (110D) slab shows that both two-coordinated and three-coordinated oxygen atoms surface states are shifted. Contrary to the (100) surface, the analysis of the valence band after optimization shows that there is a significant change in the electronic DOS related to the disappearance of some O−Al bonds. The change in DOS profiles shows a reverse trend: starting from distinct peaks in the valence band, after relaxation there is a narrowing of the valence band indicating that the chemical bonds are more uniform in the surface layers. These results support the reconstruction observed on the surface and the change in coordination of bulk aluminum atoms.

Considering the above, we concluded that relaxation is more important in the case of the (110D) slab than of the (100) slab,

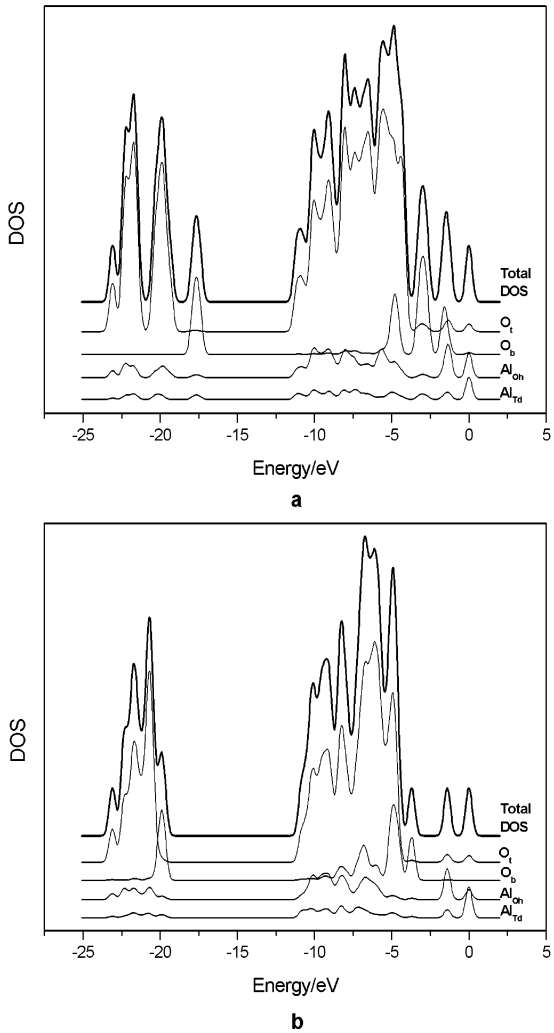

Figure 5. Electronic density of states plots of (a) unrelaxed and (b) relaxed (110D) γ-alumina unit cell. Total DOS (arbitrary units) and atom-resolved PDOS for bicoordinated (O_b) and tricoordinated (O_t) oxygens and octahedral (Al_{Oh}) and tetrahedral (Al_{Td}) aluminum atoms.

and consequently, the chemical reactivity of the first slab is different from the latter one. Differences are caused by the nature of atoms exposed by the two surfaces and in particular for the (110D) surface where the major impact of slab relaxation is the change in electronic distribution of the first layer octahedral aluminum atoms, which accentuates their Lewis acid nature and consequently their reactivity.

3.2. Adsorption of H_2O. On the five-layer (100) surface, we found that water was physisorbed. The water molecule is

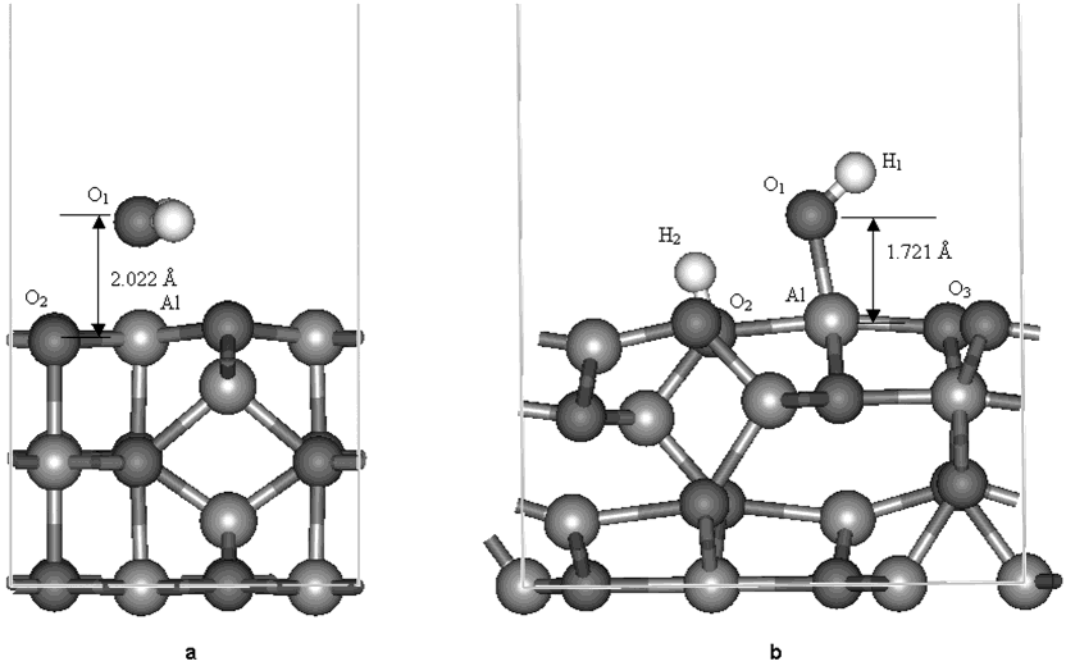

Figure 6. H_2O adsorption geometries on the (a) (100) surface and (b) (110D) surface.

adsorbed on the surface at a distance of 2.02 Å (Figure 6a). This distance is longer than that between the Al and O atoms of the surface. The bond population is 0.10 electrons, which denotes a weak interaction between the water molecule and the surface. The Mulliken population analysis shows that the charge on the molecule is +0.06 electrons, which corresponds to a weak charge transfer between the surface and the adsorbate. The charges of a single water molecule are −1.09 electrons on the O atom and +0.55 electrons on the H atoms. The equivalent charges of the adsorbed water molecule are −0.98 electrons on the oxygen and +0.52 electrons on the H atoms. We observed the same surface relaxation as in the case of the bare surface. The adsorption energy was −84 kJ/mol. The adsorbed water molecule preserves its initial geometry. The oxygen atom of the water molecule is positioned on a vertical axis to the Al site; the O_1-Al-O_3 angle is 90°. The bond lengths between O_1 and H atoms are 0.976 and 0.975 Å. The $H-O_1-H$ angle is 107.9°. The optimization of water in an equivalent cell at the same level of theory yields an O−H distance of 0.972 Å and an H−O−H angle of 104.9°. Figure 7a shows the total DOS of the system; a comparison with Figure 3b shows two extra peaks, at −9.758 and −21.788 eV, that belong to the physisorbed water molecule. The electronic structure of a single water molecule exhibits four peaks: two close peaks situated between 0 and 2 eV, one peak at −6 eV, and one at −17 eV. The presence of well-defined water peaks would support the assumption that adsorption consists of a weak interaction between water and alumina surface

On the four-layer (110D) surface, we found that water was dissociated. The dissociation energy was −272 kJ/mol. The equilibrium geometry shows a hydroxyl group bonded to the Al atom at 1.687 Å above the surface. The bond population between the Al site of the surface and the oxygen atom of the hydroxyl group is 0.53 electrons, which implies a strong covalent interaction. The O_1-H_1 bond (Figure 6b) of the hydroxyl group is 0.965 Å. The total charge on the hydroxyl group obtained on the surface is −0.65 electrons. The two-coordinated oxygen atom adjacent to the aluminum site is protonated. The proton is situated in the symmetry plane of the surface. The calculated charge on the proton is 0.49 electrons, and the distance between

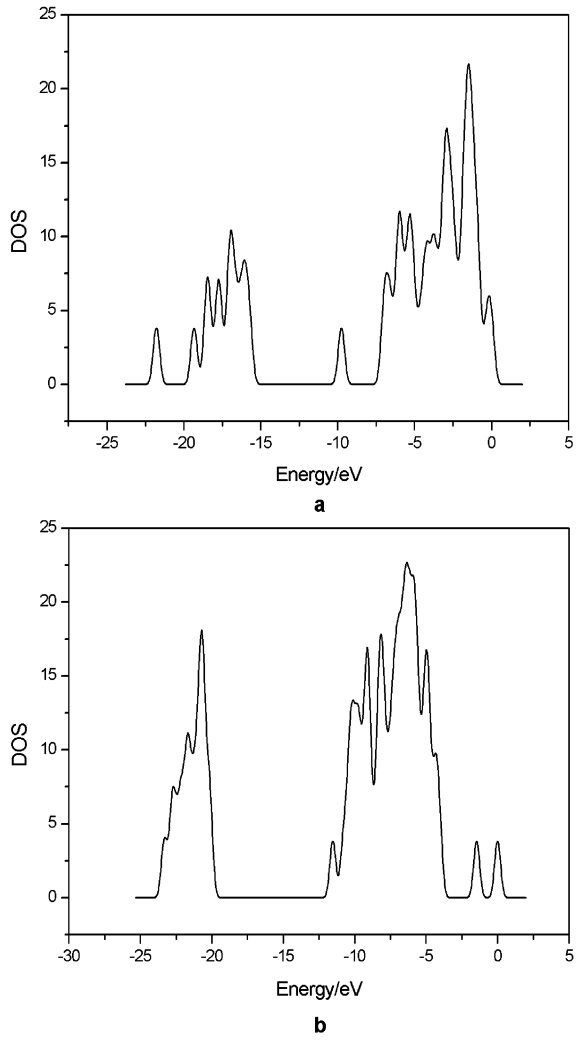

Figure 7. Total DOS (arbitrary units) of H_2O adsorbed on the (a) (100) surface and (b) (110D) surface.

that oxygen and the proton is 0.978 Å. The electronic structure of the system is shown in the Figure 7b. The peaks of the

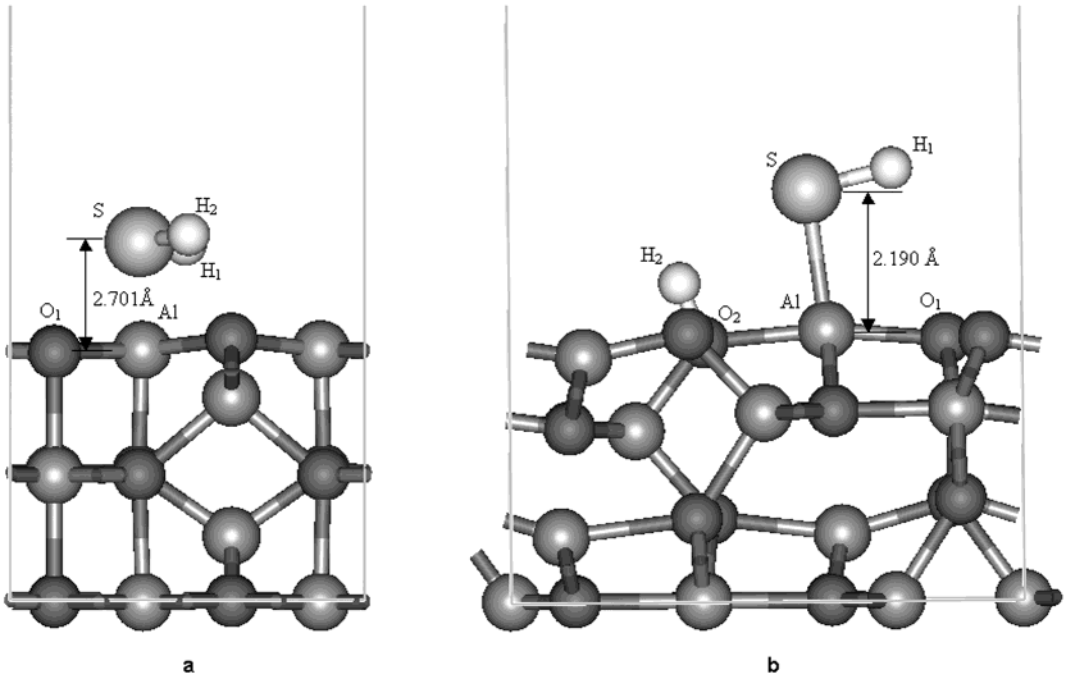

Figure 8. H_2S adsorption geometries on the (a) (100) surface and (b) (110D) surface.

isolated water molecule can no longer be recognized as a consequence of water dissociation. The strong interaction between water and the surface is sustained by the absence of isolated water molecule peaks. The peak at −11.523 eV is assigned to the new O−H bond formed after the dissociation of water.

We also did some calculations on a six-layer stoichiometric (110D) surface. The surface was held fixed while only the position of the adsorbate was optimized. We found that the water molecule dissociated on the surface similarly to the dissociation on the four-layer nonstoichiometric surface. The dissociation energy was −241 kJ/mol.

3.3. Adsorption of H_2S. On the five-layer (100) surface, the H_2S molecule as well as the three upper layers were relaxed while the two bottom layers were frozen. We found that H_2S was physisorbed on the surface aluminum site with an adsorption energy equal to −37 kJ/mol, half the adsorption energy of water on the same surface. The hydrogen sulfide molecule was adsorbed at a distance of 2.701 Å from the aluminum site. Optimization of the isolated H_2S molecule at the same level of theory yielded a value of 1.342 Å for the S−H bond length and a value of 91.79° for the H−S−H angle. The equilibrium geometry (Figure 8a) of the adsorbed H_2S molecule shows that the S−H bond length is 1.344 Å and the H−S−H angle is 92.39°. The charge on the S atom increases from −0.43 (isolated molecule) to −0.32 electrons (adsorbed molecule). The bond order between the S atom and the Al site on the surface is 0.11 electrons. All these results show that there is negligible interaction between the H_2S and the γ-alumina surface. Figure 9a shows the electronic structure of hydrogen sulfide adsorbed on the alumina surface system. The peak that appears in the energy gap is attributed to hydrogen sulfide and corresponds to a weak interaction between the molecule and the surface. The calculated DOS of a single H_2S shows four peaks: three close peaks situated between +0 and −5 eV and one peak at −12 eV.

On the four-layer (110D) surface, we found that the hydrogen sulfide was dissociated. The dissociation energy was −203 kJ/mol. The Al−S bond length is 2.190 Å. As in the case of water dissociation, the two-coordinated adjacent oxygen is protonated. The proton is situated at a distance of 0.975 Å and has a charge

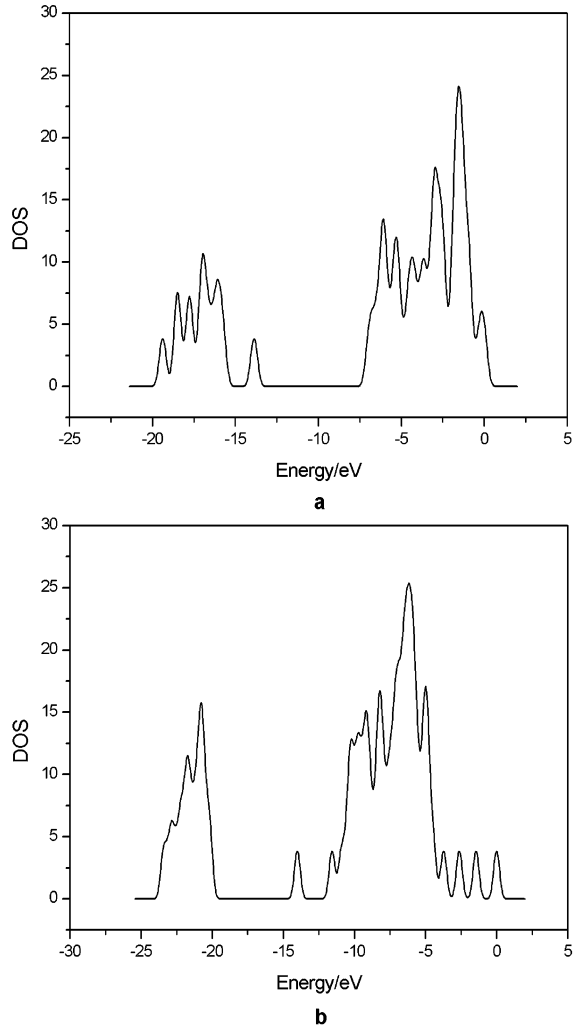

Figure 9. Total DOS (arbitrary units) of H_2S adsorbed on the (100) surface and (b) (110D) surface.

of 0.49 electrons. The proton as well as the sulfanyl group are situated in the symmetry plane of the surface (Figure 8b). The sulfanyl group is charged with −0.46 electrons, and the H−S bond length is 1.339 Å. The surface generally maintains the same equilibrium geometry as the bare optimized surface. The only difference is the slight displacement of aluminum surface sites above the oxygen atoms of the first layer as observed for the water dissociation. The electronic structure shown in Figure 9b sustains the dissociation of the molecule by the presence of hydrogen sulfide peaks shifted toward the valence band of alumina. The peak at −11.562 eV is clearly noticeable; it corresponds to the new O−H bond formed on the surface as previously seen for water dissociation.

On the six-layer stoichiometric fixed (110D) surface, we obtained a dissociation energy of −189 kJ/mol which differs by 5% from the value obtained in the corresponding case on the four-layer fixed surface. The results obtained on the six-layer surfaces for the two molecules proved that (i) a larger surface had an equivalent effect on the adsorbates (water and hydrogen sulfide) and (ii) the vacancies imposed in the bottom layer had a slight influence on the reactivity of the surface atoms reflected on the values obtained for the dissociation energy.

4. Discussion and Conclusion

In this work, we studied the adsorption of water and hydrogen sulfide on two representative surfaces of γ-alumina (100) and (110D). Reactivity on the surfaces was modeled by considering different layers of atoms. We found that both molecules were adsorbed on the (100) slab and that both molecules were dissociated on the (110D) slab. Population analysis shows that on the (100) surface the molecules were physisorbed. On the (110D) surface, the four-coordinated octahedral aluminum site dissociates the two molecules and protonation is observed on the adjacent oxygen atom. Both hydroxyl and sulfanyl groups are strongly bonded to the surface. As a consequence, the reactivity depends on the crystallographic plane. We discovered that the relaxation of the two surfaces was different. The (100) surface was more rigid, and there were minor perturbations of the superficial layer. This result is supported by previous molecular dynamic studies[29,28] which have clearly established that for the (100) surface the structure is preserved and only some oxygen atoms move slightly above the surface. On the contrary, the (110D) surface relaxation was more important; the first layer was found to be more disordered, and there was even a reconstruction of innerlayer atoms. Previous MD[30] and DFT-PW[34] calculations reported an important reconstruction of the (110) surface coupled with the loss of Al from tetrahedral cation positions. These vacancies occur on the energetically preferred (110C) surface. On the (110D) surface, there is clearly a strong intra and interlayer relaxation that leads to a significant change in reactivity in comparison with the (100) surface. This change in reactivity could be explained by the variation of the bond length between aluminum atoms and oxygen atoms, insofar as this variation alters the covalent/ionic bond character. These facts are supported by the electronic structure profiles that showed a shift of the Fermi energy level and an important modification of the band gap distance which could account for the high reactivity of the (110D) surface.

Table 4 summarizes the adsorption/dissociation energies found. For the water molecule, we found two energy minima corresponding to −84 (adsorption) and −241 kJ/mol (dissociation). The domain of experimental adsorption energies of water on γ-alumina extend from 40 to 300 kJ/mol depending on the experimental conditions or the experimental method. Our result

TABLE 4: Calculated Adsorption Energies and Experimental Heats of Adsorption (kJ/mol)

	adsorption energies			
	fixed surface		optimized surface	
surface models	H_2O	H_2S	H_2O	H_2S
ideal (100) stoichiometric slab	−94	−49	−84	−37
ideal (110D) nonstoichiometric slab	−268	−199	−272	−203
defect (110D) stoichiometric slab	−241	−189		
experiment	H_2O		H_2S	
heat of adsorption	190[19]		120[22]	

on the (100) surface is in good agreement with the value of −83 kJ/mol, which corresponds to the initial adsorption heat for physisorbed water[49] obtained by microcalorimetric experiments. As for the (110D) surface, our value is in good agreement with the experimental heat of adsorption for chemisorbed water of 190 kJ/mol.[24] Experimental studies cannot distinguish between the adsorbent plane nor identify the reactive surface atoms. The experimental energies are mean values resulting from many different contributions. Besides, the complexity of the surfaces and the diverse nature of adsorbed hydroxyls make very difficult to assign an energy value to a specific adsorption geometry. Adsorption energy values derived from theoretical studies vary from −54[35] to −564 kJ/mol.[37] Both results were obtained by quantum chemical methods on clusters that modeled different surface sites. The difference in energy values could be attributed to the cluster model: ref 35 used clusters terminated by hydrogen ions, and the latter ref 37 used clusters embedded in a set of point charges. The dissociation of water on the ideal (110D) surface differs from our previous study of H_2O on clusters of alumina.[8] Dissociative adsorption of H_2O on α-alumina, in the absence of defects, was also predicted by first-principles molecular dynamics investigations:[50] dissociative adsorption is more favorable than molecular adsorption by 10 kcal mol^{-1} and is primarily heteroclitic; that is, the OH^{-1} binds to the Al site and the proton (H^+) binds to a nearby surface O.

Our periodical model, even if it considers only four- to six-layer surfaces, makes use of crystal symmetry to provide a better representation of the alumina surface which influences the quality of adsorption sites description. Moreover, a cluster method involves hypotheses on the chemical nature of the substrate: one can choose a pure covalent model or a pure ionic model. The periodic DFT-PW model, applied here, is therefore more ab initio because the electrostatic behavior is derived from the calculations. Besides, our model does not suffer from border effects related to finite cluster termination.

For hydrogen sulfide, we found two energy minima: on the (100) surface −37 kJ/mol (adsorption) and on the (110D) surface −189 kJ/mol (dissociation). These energy values are lower than corresponding values obtained for water adsorption and are caused by the weak polarization of H_2S compared to H_2O. Experimentally,[27] the initial heat of adsorption for hydrogen sulfide on γ-alumina is 130 kJ/mol. Again, it is difficult to ascribe this experimental value to a specified adsorption geometry: although some studies[51] have considered that H_2S is fixed on the Lewis acid site of the surface, some other studies[52] have suggested an hydrogen brigded interaction between H_2S and alumina surface hydroxyls. Our model did not consider an hydroxylated surface, and we practically neglected the presence of vacancies in the slab structures. However, the results obtained are consistent with our previous[8] paper which investigated the adsorption of H_2S on representative clusters of alumina surfaces.

Table 4 also shows the energies obtained on the fixed surfaces. There is good agreement between the values obtained

on the fixed and on the optimized perfect surfaces. As for the stoichiometric (110D) slab, the differences in energy in comparison with the nonstoichiometric slab could be explained by the introduction of two vacancies in the bottom layer which influenced the electronic density of the surface layers and consequently their reactivity. We must underline that the stoichiometric surface was not reoptimized because of practical constraints. and this certainly influenced the calculated adsorption energies.

Our results showed that γ-alumina reactivity depended on the terminating layers exposed by each surface and that was directly related to the degree of distortion of the surface in the presence of the adsorbates. We will use these results as the starting point for the study we have planned on the interaction between MoS_2 crystallites and γ-alumina surfaces.

Acknowledgment. We would like to acknowledge the TotalFinaElf company for their support. The computations were done at the "Centre Régional de Compétence en Modélisation Moléculaire de Marseille."

References and Notes

(1) Poisson, R.; Brunelle, J.-P.; Nortier, P. In *Alumina, Catalysts Supports and Catalysts*; Stiles, A. B., Eds.; Butterworths: Boston, 1987.
(2) Massoth, F. E. *Advances in Catalysis*; Academic Prets, New York, 1978; Vol. 37.
(3) Gates, B. C.; Katzer, J. R.; Schuit, G. C. A. *Chemistry of Catalytic Processes*; McGraw-Hill: New York, 1979.
(4) Knözinger, H.; Ratnasamy, P. *Catal. Rev.-Sci. Eng.* **1978**, *17*, 31.
(5) Hayden, T. F.; Dumesic, J. A. *J. Catal.* **1987**, *103*, 366.
(6) Diemann, E.; Weber, T.; Müller, A. *J. Catal.* **1999**, *148*, 288.
(7) Topsøe, H.; Clausen, B. S.; Massoth, F. E. *Hydrotreating catalysis: Science and Technlogy*; Springer-Verlag: Berlin, 1991.
(8) Maresca, O.; Allouche, A.; Aycard, J. P.; Rajzmann, M.; Clemendot, S.; Hutschka, F. *J. Mol. Struct. (THEOCHEM)* **2000**, *505*, 81.
(9) Maresca, O. Ph.D. Thesis, University Lille, Lille, France, 2000.
(10) Wyckoff, R. W. G. *Crystal Structures*; Interscience Publishers: New York, 1968.
(11) Lippens, B. C.; Steggerda, J. J. *Physical and Chemical Aspects of Adsorbents and Catalysts*; Linsen, B. G., Ed.; Academic Press: London, 1970.
(12) Wang, J. A.; Bokhimi, X.; Morales, A.; Novaro, O.; Lopez, T.; Gomez, R. *J. Phys. Chem. B* **1999**, *103*, 299.
(13) John, C. S.; Alma, N. C. M.; Hays, G. R. *App. Catal.* **1983**, *6*, 341.
(14) Lee, M.-H.; Cheng, C.-F.; Heine, V.; Klinowski, J. *Chem. Phys. Lett.* **1997**, *265*, 673.
(15) Zhou, R.-H.; Snyder, R. L. *Acta Crystallogr.* **1991**, *B47*, 617.
(16) Wolverton, C.; Hass, K. C. *Phys. Rev. B* **2000**, *63*, 24102.
(17) Gutiérez, G.; Taga, A.; Johansson, B. *Phys. Rev. B* **2002**, *65*, 12101.
(18) Topsøe, N. *J. Catal.* **1980**, *64*, 235.
(19) Tsyganenko, A. A.; Mardilovich, P. P. *J. Chem. Soc., Faraday Trans.* **1996**, *92*, 4843.
(20) Beaufils, J.; Barbaux, Y. *J. Chem. Phys.* **1981**, *78*, 347.
(21) Coster, D. J.; Blumenfeld, A. L.; Fripiat, J. J. *J. Phys. Chem.* **1994**, *98*, 6201.
(22) Coster, D. J.; Fripiat, J. J.; Muscas, M.; Aroux, A. *Langmuir* **1995**, *11*, 2615.
(23) Peri, J. B. *J. Phys. Chem.* **1965**, *69*, 220.
(24) Hendriksen, B. A.; Pearce, D. R.; Rudham, R. *J. Catal.* **1972**, *24*, 82.
(25) Manchado, M.; Guil, J.; Masiá, A.; Paniego, A.; Menayo, J. *Langmuir* **1994**, *10*, 685.
(26) Zecchina, A.; Platero, E. C.; Arean, C. O. *J. Catal.* **1987**, *107*, 244.
(27) Meyer, C.; Bastick, J. *Bull. Soc. Chim. France* **1979**, *11/12*, 463.
(28) Alvarez, L. J.; Fernández Sanz, J.; Capitán, M. J.; Odriozola, J. A. *Chem. Phys. Lett.* **1992**, *192*, 463.
(29) Blonski, S.; Garofalini, S. H. *Surf. Sci.* **1993**, *295*, 263.
(30) Alvarez, L. J.; León, L. E.; Fernández Sanz, J.; Capitán, M. J.; Odriozola, J. A. *J. Phys. Chem.* **1995**, *99*, 17872.
(31) Nagy, L. T.; Micov, M.; Benco, L.; Liška, M.; Mach, P.; Tunega, D. *Int. J. Quantum Chem.* **1998**, *70*, 341.
(32) Kawakami, H.; Yoshida, S. *J. Chem. Soc., Faraday Trans. 2* **1985**, *81*, 1117.
(33) Fleisher, M. B.; Golender, L. O.; Shimanskaya, M. V. *React. Kinet. Catal. Lett.* **1987**, *34*, 137.
(34) Sohlberg, K.; Pennycook, S. J.; Pantelides, S. T. *J. Am. Chem. Soc.* **1999**, *121*, 10999.
(35) Lindblad, M.; Pakkanen, T. A. *Surf. Sci.* **1993**, *286*, 333.
(36) Pacchioni, G.; Rosch, N. *Surf. Sci.* **1994**, *286*, 333.
(37) Fernández Sanz, J.; Rabaâ, H.; Poveda, F. M.; Márquez, A. M.; Calzado, C. J. *Int. J. Quantum Chem.* **1998**, *70*, 359.
(38) DeVito, D. A.; Gilardoni, F.; Kiwi-Minsker, L.; Morgantini, P.-Y.; Porchet, S.; Renken, A.; Weber, J. *J. Mol. Struct. (THEOCHEM)* **1999**, *469*, 7.
(39) Faye, P.; Payen, E.; Bougeard, D. *J. Catal.* **1998**, *179*, 560.
(40) Räty, J.; Suvanto, M.; Hirva, P.; Pakkanen, T. A. *Surf. Sci.* **2001**, *492*, 243.
(41) Okamoto, Y.; Imanaka, T. *J. Phys. Chem.* **1988**, *92*, 7102.
(42) Chen, Y.; Zhang, L. *Catal. Lett.* **1992**, *12*, 51.
(43) Perdew, J. P.; Wang, Y. *Phys. Rev.* **1992**, *B46*, 6671.
(44) White, J. A.; Bird, D. M. *Phys. Rev.* **1994**, *B50*, 4954.
(45) Kleinman, L.; Bylander, D. M. *Phys. Rev. Lett.* **1982**, *48*, 1425.
(46) Monkhorst, H.; Pack, J. *Phys. Rev.* **1976**, *13B*, 5188.
(47) Monkhorst, H.; Pack, J. *Phys. Rev.* **1977**, *16B*, 1748.
(48) Milman, V.; Winkler, B.; White, J.; Pickard, C.; Payne, M.; Akhmatskaya, E.; Nobes, R. *Int. J. Quantum Chem.* **2000**, *77*, 895.
(49) Funini, B.; della Gatta, G.; nd D. Mazza, G. G.; Vallino, M.; Busca, G.; Ramis, G. *J. Catal.* **1978**, *24*, 82.
(50) Hass, K. C.; Schneider, W. F.; Curioni, A.; Andreoni, W. *J. Phys. Chem. B* **2000**, *104*, 5527.
(51) Rosset, A.; Finstrom, C.; Adams, C. *J. Catal.* **1962**, *1*, 235.
(52) Glass, R.; Ross, R. *J. Phys. Chem.* **1973**, *77*, 2576.